Vlasov-Maxwell simulations of high-frequency longitudinal waves in a magnetized plasma

Francesco Califano[1,2] and Maurizio Lontano[1]
[1]*Istituto di Fisica del Plasma, Consiglio Nazionale delle Ricerche, Euratom-ENEA-CNR Association, Milan, Italy*
[2]*Dipartimento di Fisica and INFM, Università di Pisa, Pisa, Italy*
(Received 14 November 2002; published 8 May 2003)

The plasma response to the injection of a propagating purely electrostatic wave of finite amplitude is investigated by means of a kinetic code which solves the Vlasov equations for electrons and ions in the three-dimensional (one spatial and two in velocity, 1D2V) phase space, self-consistently coupled to the Maxwell equations. The plasma is uniformly magnetized, and the wave frequency close to the cold upper-hybrid resonance $\omega_0=\sqrt{\omega_{pe}^2+\omega_{ce}^2}$ is considered. Coherent structures are formed in the phase space that would be completely missed by a hydrodynamic analysis. In particular, in the early stage of the interaction, the initially unperturbed equilibrium electron distribution is strongly affected as a whole by the pump, taking a ringlike shape in the velocity plane transverse to the magnetic field. Then, a sort of instability occurs, leading to the broadening and flattening of the electron distribution.

DOI: 10.1103/PhysRevE.67.056401 PACS number(s): 52.35.Hr, 52.35.Mw, 52.40.Db, 52.50.Sw

I. INTRODUCTION

The physics of the propagation of electron Bernstein waves (EBW's) [1] has been investigated for a long time in connection with their potentialities in the fields of heating and current drive in a magnetically confined plasma, for fusion energy production purposes [2], as well as for astrophysical applications [3]. They are high-frequency, almost electrostatic (ES) kinetic modes of a hot magnetized plasma, which are excited by wave transformation of an extraordinary mode in the region of the cold upper-hybrid resonance [2], or as a result of the parametric decay of an electromagnetic wave [4]. Recently, renewed interest in the use of EBW's has arisen in connection with their application to reversed field pinches and spherical tori [5–8]. Generally speaking, since EBW frequencies are in the range of the electron cyclotron frequency, their propagation and absorption properties can be well described in the framework of linear and quasilinear theories. However, due to the increasing demand for radio frequency input power in large fusion machines, bearing in mind that EBW's are excited in the region of a plasma resonance, the local wave electric field can achieve large values which may trigger a nonlinear plasma response. In this work, we describe the results of Vlasov-Maxwell numerical simulations of the interaction of a driven ES wave with frequency $\omega_0 \approx \omega_{uh}$ and $k_0\rho_{Le}\approx 1$, where ω_{uh} and ρ_{Le} are the cold upper-hybrid frequency and the Larmor radius of thermal electrons, respectively. The pump is taken in the form of a purely ES wave propagating perpendicularly to a uniform and stationary magnetic field. A one-dimensional slab geometry and two velocity components, those perpendicular to the magnetic field, are considered. A fully nonlinear regime of interaction is studied, where the electron quiver velocity is of the order of the thermal speed of the electrons. To our knowledge, this represents the first fully kinetic investigation, although in a simplified geometry, of the magnetized plasma response to a large amplitude propagating ES wave. The physical model is presented in Sec. II. The macroscopic plasma response is discussed in Sec. III; Sec. IV is devoted to the presentation of the resulting electron distribution function (EDF). A short summary and concluding remarks are given in Sec. V.

II. THE MODEL

The present investigation is based on a fully kinetic model [9] of a magnetized electron-ion plasma under the action of an externally applied ES wave. Coulomb collisions are neglected. The nonrelativistic Vlasov equations for electrons and protons are numerically integrated together with the Maxwell equations for the self-consistent electric and magnetic fields [10]. With reference to a physical system characterized by one spatial dimension (x) and two velocity degrees of freedom (v_x, v_y), and completely uniform in the y,z plane, the relevant equations are written:

$$\frac{\partial f_a}{\partial t}+v_x\frac{\partial f_a}{\partial x}-\Lambda_a\left\{[E_x(x,t)+E_{dr}(x,t)+B_z(x,t)v_y]\frac{\partial f_a}{\partial v_x}+[E_y-B_z v_x]\frac{\partial f_a}{\partial v_y}\right\}=0, \tag{1}$$

$$\frac{\partial E_x}{\partial x}=\int\int dv_x dv_y f_i(x,v_x,v_y,t)-\int\int dv_x dv_y f_e(x,v_x,v_y,t), \tag{2}$$

$$\frac{\partial E_y}{\partial t}=-\frac{\partial B_z}{\partial x}-\int\int dv_x dv_y v_y f_i(x,v_x,v_y,t)+\int\int dv_x dv_y v_y f_e(x,v_x,v_y,t), \tag{3}$$

$$\frac{\partial B_z}{\partial t}=-\frac{\partial E_y}{\partial x}, \tag{4}$$

with periodic boundary conditions, in the interval $x\in[0,6\lambda_0]$, where λ_0 and $k_0=2\pi/\lambda_0$ are the wavelength and the wave vector of the pump field, respectively. An external

uniform and constant magnetic field $\mathbf{B}_0 = B_0 \mathbf{e}_z$ is applied at $t=0$. During the evolution of the system the continuous feeding of the ES wave, propagating along the positive x direction, i.e.,

$$\mathbf{E}_{dr} = a \sin(k_0 x - \omega_0 t)\mathbf{e}_x , \tag{5}$$

causes the generation of the self-consistent field components E_x, E_y, B_z. In Eqs. (1)–(5) dimensionless variables have been used according to the following substitutions: $\omega_{pi} t \rightarrow t$, $\mathbf{v}/c \rightarrow \mathbf{v}$, $\omega_{pi}\mathbf{r}/c \rightarrow \mathbf{r}$, $f_a c^2/n_{a0} \rightarrow f_a$, $e\mathbf{E}(\mathbf{B})/m_i c \omega_{pi} \rightarrow \mathbf{E}(\mathbf{B})$. Moreover, $\Lambda_i = -1$ and $\Lambda_e = m_i/m_e = 1836$.

The aim of the present investigation is to study the nonlinear wave-plasma interaction occurring when a large amplitude ES wave propagates close to a resonance in a magnetized plasma. Specifically, we have chosen a propagating longitudinal wave with a frequency close to the upper-hybrid resonance $\omega_0 = \omega_{uh} = \sqrt{\omega_{pe}^2 + \omega_{ce}^2}$, and a wave vector such that $k_0 \rho_{Le} \approx 1$. Here, ω_{pe} and ω_{ce} are the plasma and cyclotron frequencies of the electrons, respectively, and ρ_{Le} is the Larmor radius of thermal electrons. For a low-density ($n_e = 10^{11}$ cm^{-3}), low-temperature ($T_e = T_i = 10$ eV), magnetized ($B_0 = 1$ kG) plasma, we have the following values of the dimensionless parameters: $\lambda_{De} \approx 1.03 \times 10^{-4}$, $\lambda_0 \approx 6.58 \times 10^{-4}$, $\rho_{Le} \approx 1.05 \times 10^{-4}$, $\rho_{Li} \approx 4.48 \times 10^{-3}$, $\omega_0 = \omega_{uh} = 60$, $\omega_{ce} \approx 42.2$, $\omega_{ci} \approx 0.023$. The phase velocity of the pump wave, $v_\varphi \approx 6.3 \times 10^{-3}$, corresponds to a refractive index of $N_\perp \approx 159$ ($k_0 = 9.5 \times 10^3$), such that $k_0 \rho_{Le} \approx 1$. Moreover, $\beta_e = T_e/m_e c^2 \approx 2 \times 10^{-5}$, $\beta_i = T_i/m_i c^2 \approx 1.1 \times 10^{-8}$. Finally, the electric field amplitude of the pump has been taken as 2 kV/cm, in such a way that the ratio of the ES to the electron thermal energies is close to unity. It corresponds to $a = 3 \times 10^{-4}$.

III. THE NUMERICAL RESULTS

In order to characterize the macroscopic properties of the plasma under the action of the applied ES wave, let us examine first the space-time behavior of the hydrodynamic quantities associated with the electron and ion populations. In Fig. 1 the x component of the electric field E_x (a), the electron density n_e (b), and the ion density n_i (c) are shown as functions of time t, at the spatial location $x = 0.0021$. Here, the normalized pump frequency is $\omega_0 = 60$ and the field amplitude is $a = 3 \times 10^{-4}$. The electron density manifests quite regular oscillations of the order of $\pm 20\%$ of the unperturbed value. The ion density is perturbed to a less extent and shows a slow transient dynamics in response to the sudden initial appearance of the wave perturbation. We notice that the electron response (b) is harmonic where the ion perturbation is smaller (that is, for $t > 1.5$), while it has a nonregular character where the ion density is more heavily perturbed (for $t < 1.5$).

In Fig. 2, the average electron "temperature" T_x (a) in the x and T_y (b) in the y direction, defined as $\langle T_{x(y)} \rangle_x \equiv \langle \langle [v_{x(y)} - \langle v_{x(y)} \rangle_{\mathbf{v}}]^2 \rangle_{\mathbf{v}} \rangle_x$ (that is, normalized to the initial temperature T_e, and averaged over the spatial coordinate), are plotted as functions of time t. Figure 2 shows the achievement of a quasistationary state in which the electron

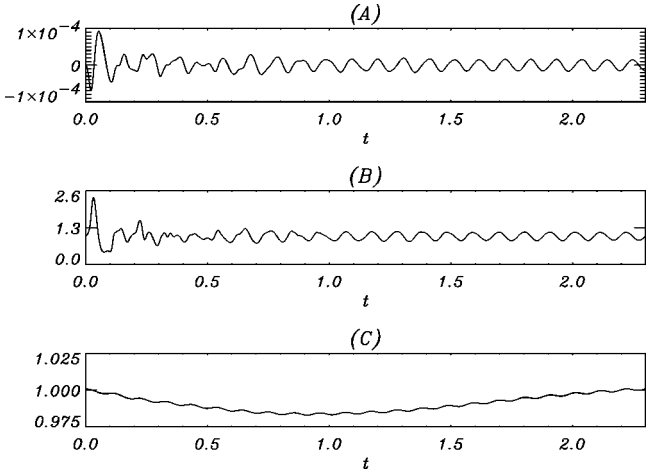

FIG. 1. E_x (a), n_e (b), and n_i (c) are shown as functions of t, at $x = 0.0018$, for $\omega_0 = 60$ and $a = 3 \times 10^{-4}$.

energy is increased by an order of magnitude. Moreover, it is seen that, although in the transient phase ($t < 1$) appreciable anisotropies can occur, the energy gain on longer time scales, averaged over space, proceeds with the same rate on the two degrees of freedom transversely to $\mathbf{B}_0$. However, at a given position, the EDF still manifests its anisotropy at all times, as discussed below.

The frequency spectra of the electric field $|E_\omega|^2$ (a), of the electron density perturbation $|n_{e,\omega}|^2$ (b), and of the ion density perturbation $|n_{i,\omega}|^2$ (c) averaged over the integration range $x \in [0, 6\lambda_0]$, are displayed in Fig. 3. Here, the peaks at $\omega_{ce} \approx 42.2$, at $\omega_0 = 60$, and at its lowest-order harmonics ($2\omega_0 \approx 120$, $3\omega_0 \approx 180$) can be seen.

From the above figures it appears that, for a pump frequency of 60, the plasma response turns out to be basically linear for the ion component, while it manifests a nonlinear behavior as far as the electrons are concerned.

We now turn to the description of the time evolution of

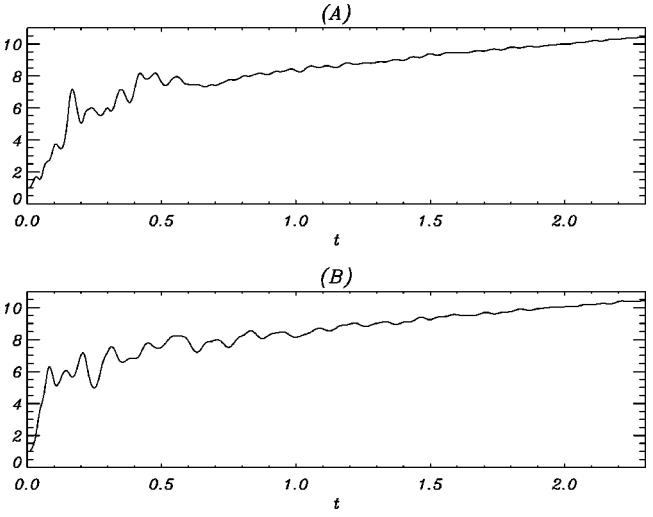

FIG. 2. The electron temperature along x (a) and along y (b) $\langle T_{e,x(y)}(x,t) \rangle_x$, averaged over $x \in [0, 6\lambda_0]$, is plotted versus time, for $\omega_0 = 60$ and $a = 3 \times 10^{-4}$.

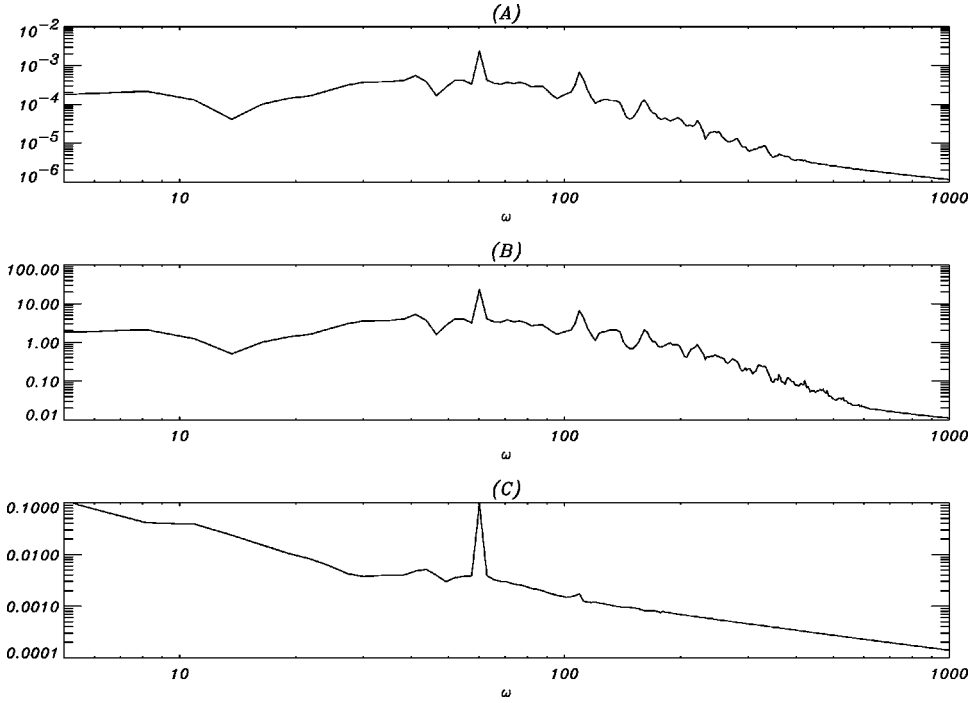

FIG. 3. The frequency spectra of $|E_\omega|^2$ (a), $|n_{e,\omega}|^2$ (b), and $|n_{i,\omega}|^2$ (c), averaged over the integration range $x\in[0,6\lambda_0]$, are shown as functions of ω.

the EDF under the action of the propagating ES wave, which represents the principal outcome of a kinetic analysis.

The numerical integration of the relevant system of equations allows us to compute the temporal evolution of the EDF $f_e(x,v_x,v_y)$. In order to have a full picture of the physics resulting from our simulations, we shall base our discussion on three different representations of the EDF (see Fig. 4): (i) the contour plots of $f_e(x,v_x,v_y)$ in the velocity space (v_x,v_y), at a given spatial position $x=2.5\times10^{-3}$ (a)–(c),(e); (ii) the contour plots of $f_e(x,v_x,v_y)$ in the phase space (x,v_x), at $v_y=0$ and $x=2.5\times10^{-3}$ (d); (iii) the contour plots of $\langle f_e(x,v_x,v_y)\rangle_x$, which is spatially averaged over $x\in[0,6\lambda_0]$, in the velocity space (v_x,v_y) (f).

The contour plots of the EDF in the velocity space (v_x,v_y) are shown at subsequent times $t=0$ (a), $t=0.1$ (b), and $t=0.16$ (c). Notice that the normalized times corresponding to an electron cyclotron period and to a wave period are $t_c=2\pi/\omega_{ce}\approx0.15$ and $t_0=2\pi/\omega_0\approx0.1$, respectively. Initially, for $t<t_0$, the bulk of the EDF undergoes at the same time a ''rotation'' and a ''diffusion'' in pitch angle, due to the mismatch between ω_0 and ω_{ce}, producing an annular structure in the velocity space. At subsequent times $(0.1<t<0.6)$, the system goes through a phase characterized by a multipeaked EDF [see, for example, plot (c)], during which different parts of the velocity plane mix up, leading to an increase of the typical width of the EDF. Notice that this part of the temporal evolution corresponds to the irregular fluctuations of the electric field and of the electron density displayed in Figs. 1(a) and 1(b). After several t_c's (e), a sort of instability takes place, which tends to redistribute the electrons in order to flatten and broaden the distribution function; a kind of quasistationary state is then achieved with a more regular EDF, which, however, still presents anisotropic features, which will be discussed below. The phase space (x,v_x), at $v_y=0$, is shown in Fig. 4(d). It is seen that the process of ''depletion'' of the EDF from the region around $v_x=0$, with the consequent formation of a ring-shaped distribution (the pointlike contours correspond to the section at $v_y=$const of the ''rings''), occurs during the early times of the temporal evolution $t<t_c$ (a)–(c).

A more smooth representation of this dynamics is shown by the spatially averaged EDF $\langle f_e(x,v_x,v_y)\rangle_x$ [see Fig. 4(f)]. Notice that plots (e) and (f) are taken at the same time $t=2.3$, for the sake of comparison. The spatially averaged EDF corresponds to what could be observed by means of a diagnostics of finite spatial resolution (as, for example, x rays, electron cyclotron emission, Thomson scattering, etc.). Indeed, the formation of a ringlike structure followed by a mixing in velocity space and by the achievement of a nearly (but not completely) isotropic average EDF is observed. The asymptotic behavior of the fluid plasma parameters (see Fig. 1), and of the EDF (see Fig. 4) suggests that after a few tens of electron cyclotron periods an almost stationary state is achieved by the system.

The two-dimensional distribution $f_e(v_x,v_y)$ is shown in Fig. 5, at $t=0.1$ (a), and $t=2.14$ (b), for $x=2.5\times10^{-3}$.

By inspection of Fig. 4 we can state that initally a good estimate of the energy gained by the electrons is of the order of the quiver energy $\tilde{v}^2$, where $\tilde{v}=a\Lambda_e/\omega_0\approx9.2\times10^{-3}$. After a few upper-hybrid periods, $t_{uh}=2\pi/\omega_{uh}\approx t_0\approx0.1$, collective effects begin to play a role and electrons are trapped and accelerated in the x direction before a full cyclotron orbit is completed. Notice that, due to the large amplitude of the pump, the bounce frequency is quite high, $\omega_b=(a\Lambda_e k_0)^{1/2}\approx72$, so that v_x can achieve the values of $(\omega_0+\omega_b)/k_0\approx1.4\times10^{-2}$ or even $(2\omega_0+\omega_b)/k_0\approx2\times10^{-2}$, if the excitation of the second harmonic of the pump is considered (see Fig. 3). These values well describe the ''average'' EDF in Fig. 4(f), although, locally, higher velocities can be reached.

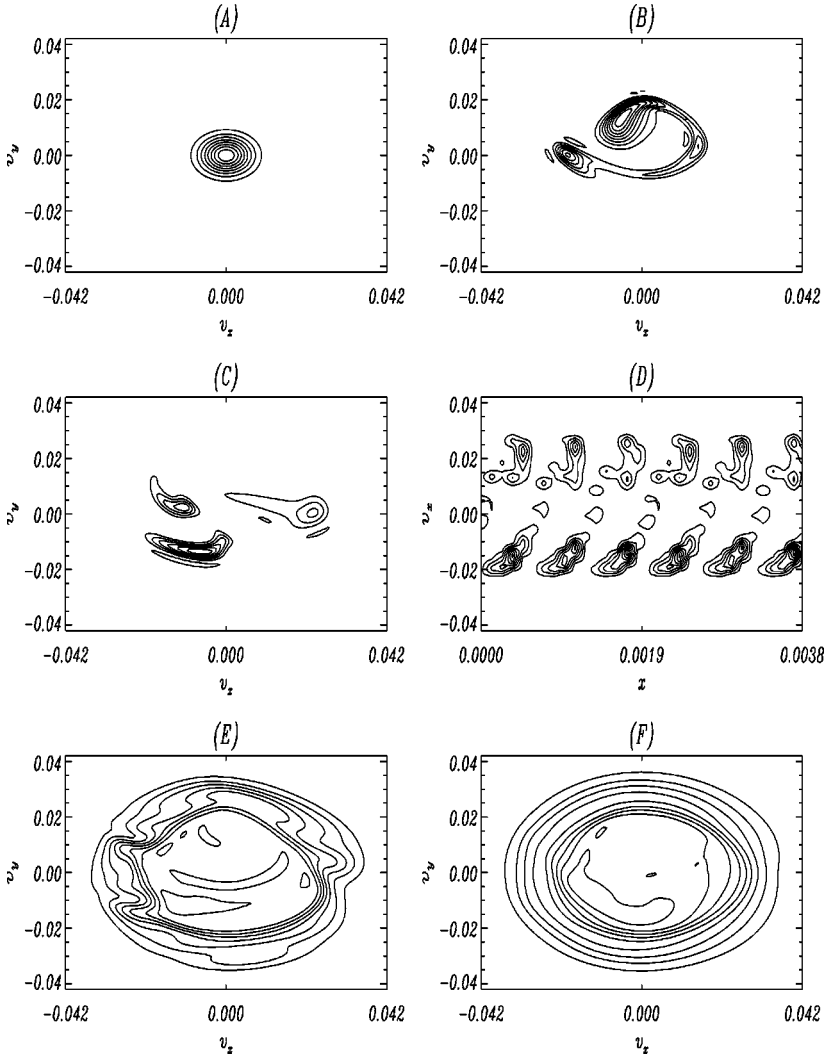

FIG. 4. The contour plots of $f_e(x,v_x,v_y)$ in the velocity space (v_x,v_y), at a given spatial position $x=2.5\times10^{-3}$, are shown at successive times: in the time intervals $t=0$ (a), 0.1 (b), 0.16 (c), and 2.3 (e). The contour plot of $f_e(x,v_x,v_y)$ in the phase space (x,v_x), at $v_y=0$, is also displayed at $t=0.16$ (d). Finally, the contour plot of $\langle f_e(x,v_x,v_y)\rangle_x$, which is spatially averaged over $x\in[0,6\lambda_0]$, in the velocity space (v_x,v_y) is shown at $t=2.3$ (f). The normalized times corresponding to a cyclotron period and to a wave period are $t_c=2\pi/\omega_{ce}\approx0.15$ and $t_0=2\pi/\omega_0\approx0.1$, respectively.

The main features of the EDF change in the course of time. In the early phase, within $3t_c$ or $4t_c$, a typical ring-shaped distribution is formed, although it may be quite irregular, giving rise to a strongly anisotropic distribution: the electrons are brought almost all together and are accelerated to $\tilde{v}$, while the Larmor rotation redistributes the acquired energy in the azimuthal angle. At later times, when a collective plasma response occurs, the EDF is widened, flattened, and made quite isotropic, up to velocities of the order of 0.02–0.025, which correspond to an increase of the electron temperature of one order of magnitude. When the quasistationary distribution is established (that is, typically, for $t>1$), some regular structures appear, which depend on the space location under consideration. They are in the form of ''tips'' in the negative-v_x part of the velocity space, and rotate counterclockwise at the Larmor angular frequency [see Fig. 4(e)]. They are absent when the spatial average of the EDF is taken [see Fig. 4(f)]. Such structures have already been observed in the kinetic simulation of ES waves around the ion cyclotron harmonics [11]. The regularity of these features, the fact that they rotate following the Larmor motion of electrons, and their existence outside the trapping region only, that is, where the charged particles do not undergo any resonant interaction, is a signature that they are a ''memory'' of the structure of the pump wave which is caused by the ballistic motion of the particles. Since these features depend on the phase of the wave, they disappear when the spatially averaged distribution is calculated.

IV. CONCLUDING REMARKS

The nonlinear interaction between a driven ES wave, propagating normally to the external uniform magnetic field, and a collisionless electron-ion plasma has been investigated by means of a Vlasov-Maxwell code. The aim has been to model the propagation of a large amplitude EBW close to the upper-hybrid resonant layer. It is shown that a high-frequency ES wave produces a ringlike EDF, characterized by a strong anisotropy in the velocity space, during the early phase of the interaction. Later on, after few cyclotron periods, the strong perturbations induced by the wave in the EDF result in the collisionless heating of the electrons and in the achievement of a quasistationary state, characterized by quite regular, harmonic oscillations of the electron density of $\pm20\%$ of its unperturbed value. These large amplitude density oscillations are supported by a strongly nonequilibrium

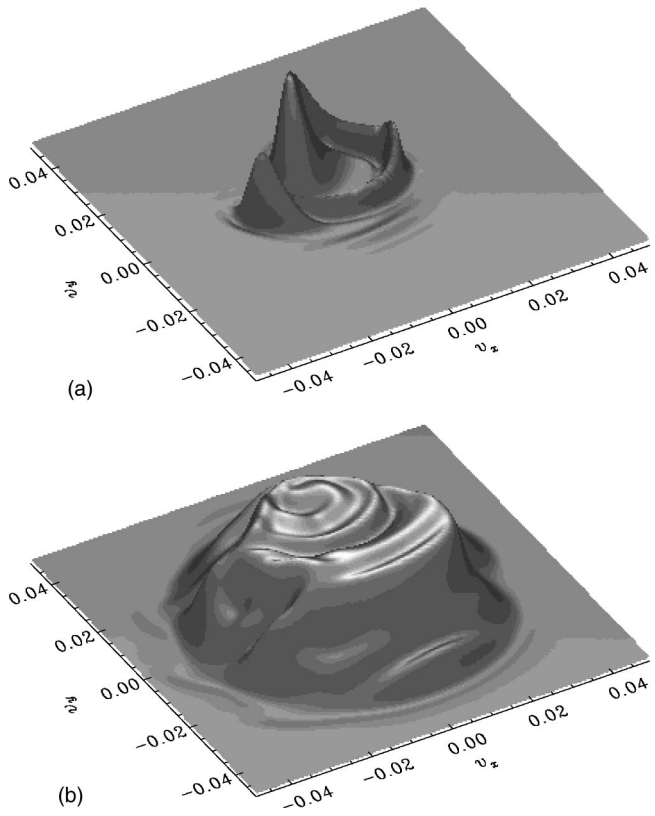

FIG. 5. The electron distribution function $f_e(v_x, v_y)$ is shown at $t=0.1$ (a) and $t=2.14$ (b) for $x=2.5\times10^{-3}$.

distribution function, which presents several interesting features. The quasistationary EDF, averaged over the spatial range of integration, is wider than the initial one, flat in the central part, and quite isotropic in the $\{v_x, v_y\}$ plane, corresponding to an increase in the electron temperature by an order of magnitude. However, locally, regular features in the negative-v_x half space appear which are related to the initial phase of the wave. They are quite stable and ''rotate'' counterclockwise according to the Larmor motion of the electrons. The occurrence of such a regular perturbation of the EDF is interpreted as the signature of the external perturbation which affects the EDF in the resonant region, but has no time to develop shorter and shorter scales in the velocity space, and to phase mix. In contrast, the Larmor rotation brings the perturbed electrons out of the trapping region so that the imprinting of the external perturbation is not canceled out, until they undergo a successive ''application'' of the wave. The effect in the long run is that the local EDF in the presence of a large amplitude ES wave manifests a dynamical structure, which remains appreciably anisotropic in the plane perpendicular to the external magnetic field all along the interaction.

The present analysis is limited to a plasma with one spatial and two velocity dimensions. The inclusion of the electron dynamics in the direction of the magnetic field would require the introduction of two more dimensions z and v_z, with a substantial increase in the computational demand. However, in the more realistic situation where a finite v_z is taken into account, we expect that the above phenomenology still takes place provided the electrons, streaming along B_0, make many cyclotron orbits before escaping from the interaction region (with typical spatial scale L_{int}). If $L_{int} \approx 5$ cm is considered, we can estimate t_{int}/t_c $(\propto L_{int}B_0/\sqrt{T_e}) \approx 10^2$, where $t_{int}=L_{int}/v_{Te}$. Therefore, if the plasma is strongly magnetized, our model looks satisfactory.

ACKNOWLEDGMENT

Part of this work was supported by the INFM Parallel Computing Initiative.

[1] I. B. Bernstein, Phys. Rev. **109**, 10 (1958).
[2] A. G. Litvak, in *High-Frequency Plasma Heating*, edited by A. G. Litvak (AIP, New York, 1992), Chaps. 1 and 7.
[3] M. Moncuquet, N. Meyer-Vernet, and S. Hoang, J. Geophys. Res. [Space Phys.] **100**, 21697 (1995).
[4] D. R. Nicholson, Phys. Fluids **27**, 650 (1984).
[5] C. B. Forest, P. K. Chattopadhyay, R. W. Harvey, and A. P. Smirnov, Phys. Plasmas **7**, 1352 (2000).
[6] A. K. Ram and S. D. Schultz, Phys. Plasmas **7**, 4084 (2000).
[7] R. A. Cairns and C. N. Lasmore-Davies, Phys. Plasmas **7**, 4126 (2000).
[8] P. K. Chattopadhyay, J. K. Anderson, T. M. Biewer, D. Craig, C. B. Forest, R. W. Harvey, and A. P. Smirnov, Phys. Plasmas **9**, 752 (2002).
[9] A. Mangeney, F. Califano, C. Cavazzoni, and P. Travnicek, J. Comput. Phys. **179**, 495 (2002).
[10] F. Califano and M. Lontano, Bull. Am. Phys. Soc. **45**(7), 332 (2000).
[11] C. Marchetto, F. Califano, and M. Lontano, Phys. Rev. E **67**, 026405 (2003).